

Composite membranes for proton exchange membrane fuel cells based on methyl methacrylate-co-maleimide/phosphotungstic acid

Zahra Seyedzadeh¹, Fariborz Atabaki^{1,*}, Negin Ghaemi², Mohammad Nasiri¹

¹ Department of Chemistry, Malek-ashtar University of Technology, Shahin-shahr, Iran

² Department of Chemical Engineering, Kermanshah University of Technology, Kermanshah, Iran

Article history:

Received: 01/Jan/2018

Received in revised form: 07/Apr/2018

Accepted: 17/May/2018

Abstract

Poly(methyl methacrylate-co-nitrophenyl maleimide) (P(MMA-co-NMI)) and poly(methyl methacrylate-co-hydroxyphenyl maleimide) (P(MMA-co-HMI)) copolymers were synthesized using free radical polymerization reaction.

Proton exchange membranes fuel cell (PEMFC) by dry-phase inversion method were fabricated using different concentrations of these copolymers and phosphotungstic acid (PWA) as an additive of the proton conductive agent.

To identify and investigate were used FT-IR, IEC, Wu, SEM, TGA, DSC, and DTG and proton conductivity (Impedance Spectroscopy) methods. Results revealed applying (P(MMA-co-HMI)) and PWA significantly improved the proton conductivity of membrane ($2.6 \times 10^{-1} \text{ S.cm}^{-1}$) due to improving the interaction between the functional groups of PWA (H_3O^+ ions, O atoms) and MMA-co-HMI copolymer (OH, C=O functional groups).

Keywords: proton exchange; membranes; PEM Fuel cell; Copolymer; Phosphotungstic acid.

1. Introduction

Fuel cells are electrochemical energy conversion devices converting chemical energy of fuels directly into electricity without combustion and suggesting superiorities in energy management, fuel sources and environmentally friendly power sources. They are attractive for commercial, residential, and military applications and are one of the most promising processes that provide clean energy and increase clean energy demand [1-5].

The polymer electrolyte membrane fuel cell is the most promising candidate system among all fuel cell systems in terms of operation mode and application [6].

Proton exchange membranes (PEMs) play a key role in fuel cell operation. In the fuel cell PEMs provide three main contributions: as ion transfer media, for separating reactant gases (hydrogen and oxygen) which react at the cathode and anode, and as a catalyst support.

In the recent scenario, proton exchange membrane fuel cell (PEMFCs) are one of the most promising clean energy technologies. PEMFCs have certain potential advantages such as portable applications, power generation, high efficiency and etc. Generally, a proton exchange membrane (PEM) should present the following properties: high proton conductivity;

*.Corresponding author: Assistant Professor of Applied Chemistry, Faculty of Chemistry, Malek Ashtar University of Technology. E-mail: atabaki@mut-es.ac.ir

high chemical and mechanical stability; low permeability of fuels; low cost; sufficient thermal stability and good film-forming capability [6-12].

Nafion is one of the most applicable polymers employed for fabrication of PEM. The hydrated Nafion membrane exhibits high proton conductivity and is applied at temperatures up to 80°C. However, there are some limitations in the application of this polymer; high cost, low conductivity due to water loss at high temperature, low humidity and high permeability to methanol, hard synthesis and environmental problems [2, 13]. Hence, many studies have been conducted to develop non-perfluoro sulfonic PEMs based on polystyrene, polyethersulfone (PES), poly(etherether ketone) (PEEK), polyphosphazene, polybenzimidazole (PBI), polyesters, poly (acrylonitrile) (PAN), polymethyl methacrylate (PMMA) and polyimides. These materials have excellent chemical resistance due to higher C-H bond strength in the benzene ring compared to aliphatic one. Other advantages of these materials include lower cost, excellent chemical resistance, and good mechanical properties [1, 10, 14].

Recently, poly(methyl methacrylate) (PMMA) has attracted much attention as an organic matrix of solid-state batteries. Since the addition of PMMA in non-aqueous gel electrolytes results in a significant increase of conductivity [15-19]. This increment is due to the content and the molecular weight of PMMA as well as the role of PMMA in dissociation of salt in gel electrolytes. Moreover, PMMA has exceptional thermal and mechanical stability as well as a compatibility with non-aqueous electrolytes [14, 20-23].

High-performance polyimide (PI) with high ionic conductivity and high mechanical and thermal properties has been considered as an alternative material to Nafion in solid electrolyte membrane fuel cells. Structural modification of polyimide membranes by embedding inorganic nanofillers (silica, titania, silquioxane, nano clay) and organic nanoparticles (graphene, graphene oxide (GO),

carbon black (CB), carbon nanotube (CNT) and phosphotungstic acid (PWA)) into the membrane matrix have also been reported by many researchers. Meanwhile, n-substituted maleimides (MI) are also known as the most important class of high performance polymers due to their thermal, electrical and mechanical properties. Hence, these polymers were employed in fabrication of high performance composites in high temperature insulators, coatings, adhesives and matrices [24-31].

In recent years, organic-inorganic hybrids have received a great deal of attention due to their advantages in improving mechanical and thermal properties as well as proton conductivity [13, 32, 33]. Among them, the hybrids doped with highly conductive heteropolyacids (HPAs) such as phosphotungstic acid (PWA) and silicotungstic acid have exhibited excellent performance and encouraging results. HPAs as a new kind of electrolytes with Keggin anion structure have been considered as one of the most conductive solids among the inorganic solid electrolytes for fabrication of composite PEMFCs membranes due to unique structure, simple preparation and strong acidity [7, 13, 34-38].

Reviewing the literature revealed that there are some reports on the synthesis of MI and PMMA, but there are currently no studies no study on employing of this copolymer for fabrication of composite membranes for proton exchange applications. It is expected, due to particular properties of PMMA and MI, the copolymer of these two polymers with appropriate functional groups improve the properties and proton conductivity of membrane. Hence, this study, in the first stage, focuses on the synthesis of poly(methyl methacrylate-co- nitrophenyl maleimide) (MMA-co-NMI). In order to improve the proton conductivity of membranes, PWA with different concentrations was added as additive into the membrane matrix. In the next stage, poly(methyl methacrylate-co-hydroxyphenyl maleimide) (MMA-co-HMI) was synthesized, and proton exchange membranes were fabricated using this copolymer without and with the

addition of different concentrations of PWA as additive into the membrane matrix. The structure and properties of synthesized polymers and membranes were studied using FTIR, SEM, TGA, DTG, DSC, IEC, water uptake and AC impedance spectroscopy and with particular emphasis on the PEM related properties, such as proton conductivity of membranes.

2. Experimental

2.1 Materials

Methyl methacrylate (MMA), ethyl acetate, benzoyl peroxide (BPO), 2-methyl-4-nitroaniline, 4-hydroxyaniline and maleic anhydride (MA), sulfuric acid, acetone, acetic anhydride and sodium acetate were purchased from Merck, Germany.

Phosphotungstic acid (PWA, $MW=2800 \text{ g mol}^{-1}$), butyl acetate (BUAc) and potassium hydroxide were supplied by Fluka, Switzerland. All of the reagents and solvents were of analytical purity grade. Non-woven sheets were received from Coin Nanotech, Aldrich, china.

2.2 Synthesis of Poly(methyl methacrylate-co-nitrophenyl maleimide) (MMA-co-NMI) Copolymers

For preparation of (MMA-co-NMI) copolymer, the solution copolymerization of MMA (6 g, 0.06 mol) and NMI (9.28 g, 0.04 mol) monomers was carried out in ethyl acetate and BPO (1 wt.%) as initiator in a 25-ml



Fig. 1 Structure of poly(MMA-co-NMI) copolymer

round-bottomed flask equipped with a condenser at a temperature of 80 °C under nitrogen atmosphere. After stirring for 6 h, the mixture was added drop wise into a large amount of methanol. Finally, in order to remove the residual solvent and to dry the produced copolymer, it was heated using a vacuum oven at 70 °C for 2 h, according to the synthesis method described elsewhere [39]. The chemical structure of MMA-co-MI copolymer is schematically shown in Fig. 1.

2.3 Synthesis of Poly(methyl methacrylate-co-hydroxyphenyl maleimide) (MMA-co-HMI) Copolymers

2.3.1 Synthesis of N-4-hydroxyphenyl maleimide

The PMMA-co-HMI copolymer was synthesized via a two-step reaction of maleic anhydride with 4-hydroxyaniline (Fig. 2). The first step, powdered maleic anhydride (4.9 g, 0.05 mol) was dissolved in

15 ml of acetone into a 25 ml round-bottomed flask equipped with a magnetic stirrer. Then, a solution of 4-hydroxyaniline (5.45g, 0.05 mol) in 15 ml of acetone was added drop wise under vigorous stirring to reach a yellow color solid. After complete addition, the mixture was stirred for 1 h, and the solid (maleamic acid) precipitated was filtered off. After drying under vacuum, the desired compound was recovered as yellow needles (yield:7.74 g, 82 %, m.p:218-221 °C). The maleamic acid (8.28 g, 0.04 mol) was dissolved in 15 ml of acetic anhydride, and then, 0.3 g of sodium acetate was added to the mixture. The mixture was heated for 6 h at 90°C under reflux. The reaction mixture slowly was poured in 150 ml of ice water and stirred for 1 h. A cream solid was recovered by filtration and drying (yield 6.73 g, 89%. m.p:251-153°C).

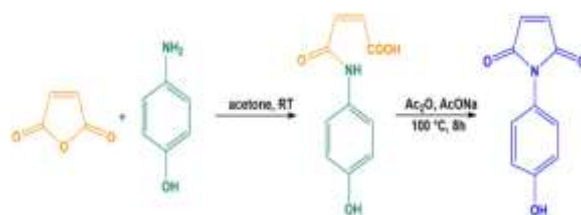


Fig. 2 Synthesis of N-4-hydroxyphenyl maleimide

2.3.2 Synthesis of (MMA-co-HMI) copolymers

For preparing of copolymers with different compositions, the solution copolymerization of MMA (6 g, 0.06 mol) and HMI (7.56 g, 0.04 mol) was carried out at 80 °C under nitrogen atmosphere in ethyl acetate according to the Fig. 3. BPO (1 wt.% based on monomers) was employed as free radical

initiator. The mixture was stirred for 6 h and then, the polymerization solution was added drop wise into a large excess of methanol. The isolated copolymer was washed with methanol, and the residual solvent of the final product was removed under vacuum at 70 °C for 2 h to yield pure white PMMA-co-HMI.



Fig. 3. Synthesis of poly(MMA-co-HMI) copolymer

2.4 Preparation of Composite Membranes

In the present work, the membranes of poly(MMA-co-NMI) and poly(MMA-co-HMI) copolymers and also composite membranes consisting of copolymers and different concentrations of PWA ((MMA-co-NMI)/PWA and (MMA-co-HMI)/PWA) were prepared via dry-phase inversion method (solvent evaporation). In this regard, solutions containing different concentrations of copolymers of poly(MMA-co-HMI) and poly(MMA-co-NMI) with solvent (BUAc), (15 and 30 wt.%) were prepared and stirred for 2 h at room temperature to reach a homogeneous solution. After that, casting solution was cast on a piece of polyester non-woven using a homemade applicator with 80 μm thickness and dried at room temperature for 24 h. In the case of preparation of membranes using different concentrations of PWA as the additive, considered an amount of PWA was measured and separately

dissolved in BUAc solvent. After ultrasonication for 10 min, desired amount of copolymer was added into the PWA solution, and similar trend was repeated for fabrication of mixed matrix membranes as mentioned above. Chemical compositions of casting solutions applied for preparation of membranes are presented in Table 1. It should be mentioned that higher amount of PWA (>1.5 wt.%) was also employed for fabrication of poly(MMA-co-HMI) composite membranes, but a heterogeneous polymeric solution was not achieved due to the high concentration of additive.

3. Characterization Methods

3.1 Fourier transform infrared (FT-IR) spectroscopy

FT-IR spectra were measured in absorbance mode using a Fourier transform infrared spectrophotometer (FT-IR, Perkin-Elmer, Shimadzu, Japan) with a temperature control cell.

The spectra were measured in the range of 700-4000 cm^{-1} and all the spectra were measured at a resolution of 4 cm^{-1}

Table 1. Composition of prepared membranes

Membrane Name	Copolymer	Copolymer amount (wt.%)	PWA (wt.%)
Poly(MMA-co-NMI)15	Poly(MMA-co-NMI)	15	0
Poly(MMA-co-NMI)30		30	
Poly(MMA-co-NMI)15/PWA1		15	1
Poly(MMA-co-NMI)30/PWA1		30	
Poly(MMA-co-HMI)15	Poly(MMA-co-HMI)	15	0
Poly(MMA-co-HMI)15/PWA0.5			0.5
Poly(MMA-co-HMI)15/PWA1			1
Poly(MMA-co-HMI)15/PWA1.5		1.5	
Poly(MMA-co-HMI)30		30	0
Poly(MMA-co-HMI)30/PWA1			1
Poly(MMA-co-HMI)30/PWA1.5			1.5

3.2 Scanning electron microscopy (SEM)

The cross-sections of prepared membranes were observed using scanning electron microscopy (SEM, KYKY-EM3200, China). The membranes were frozen in liquid nitrogen and broken. Membranes were transferred into the microscope with a sample holder after sputtering with gold as the conductive material.

3.3 Ion exchange capacity (IEC)

The ion exchange capacity (IEC) was measured via classical titration method. The dried membrane was soaked in NaCl (0.1 M) solution over night to replace all H^+ with Na^+ , and then, solution was titrated by NaOH (0.01 N) solution. IEC was calculated using the following equation [40].

$$\text{IEC} = \frac{C_{\text{NaOH}} \times V_{\text{NaOH}}}{M_{\text{sample}}} \quad (1)$$

where C_{NaOH} is concentration of NaOH solution; V_{NaOH} is volume of NaOH solution measured in the titration and M_{sample} is mass of the dry sample. It should be mentioned that IEC was measured at least two times and average amount was reported as the final value.

3.4 Water uptake

The membranes were dried in an oven at 40 °C for 48 h, weighed, soaked in deionized water overnight at room temperature. After that, surface moisture of membranes was removed by filter paper and weighed.

Water uptake was calculated from following equation [40]:

$$\text{water uptake} = \frac{W_w - W_d}{W_d} \times 100\% \quad (2)$$

In which, W_w and W_d are weight of wet and dry membranes, respectively.

3.5 Proton conductivity

The resistance of the membranes was measured using AC impedance (hioki 3560 AC mili ohm hitester-HFR meter, AHNS Co., Iran) analyzer and proton conductivity cell. The membrane sample (3cm × 4cm) was sandwiched between two Teflon parts attached with two platinum foils and two platinum wires. The impedance was measured in the frequency range of 100 kHz to 10 Hz at amplitude of 10 mV. Proton conductivity, (σ) was calculated using the following equation [15, 40].

$$\sigma(S/cm) = \frac{L}{RS} \quad (3)$$

Where L, R and S are thickness (cm), impedance (Ω) and surface area (cm^2) of membranes, respectively. It should be mentioned that the conductivity of poly(MMA-co-NMI)/PWA and poly(MMA-co-HMI)/PWA composite membranes were measured at 80 °C and 100% relative humidity (RH).

3.6 Thermal analyses

Thermogravimetric analyses (TGA), Differential thermogravimetric analyses (DTG) and

differential scanning calorimetry (DSC) diagrams were achieved by Perkin Elmer system under argon atmosphere at a heating rate of 10°C/min and over the room temperature to 700°C.

4. Results and Discussion

4.1 FT-IR Analysis

FT-IR spectra of PWA, poly(MMA-co-NMI)30 and poly(MMA-co-NMI)30/PWA1 membranes are presented in Fig. 4. In the FT-IR spectra of poly(MMA-co-NMI) copolymer, the maleimide units were identified by the appeared bands at 1782 cm⁻¹ (C=O imide stretching), 1589 cm⁻¹ (C=C aromatic stretching), 1530 cm⁻¹, and 1348 cm⁻¹ (N=O stretching) as reported in the literature [39]. The

PWA spectrum shows absorption bands at about 1080 cm⁻¹ (P-O in central tetrahedral), 985 cm⁻¹ (terminal W=O), 890 cm⁻¹ and 814 cm⁻¹ (W-O-W) associated with the asymmetric vibrations in Keggin polyanions [34, 36]. Comparing the FT-IR spectra of poly(MMA-co-NMI)30/PWA1 composite membrane with (MMA-co-NMI)30 copolymer indicates (Fig. 4) some differences in the shape and place of the appeared peaks of the spectrum which might be related to the interaction between the functional groups of copolymers (C=O and NO of NO₂) and PWA (oxygen atoms and water molecules) so that proton might be transferred by Vehicle (diffusion) mechanism and Grotthuss mechanism simultaneously.

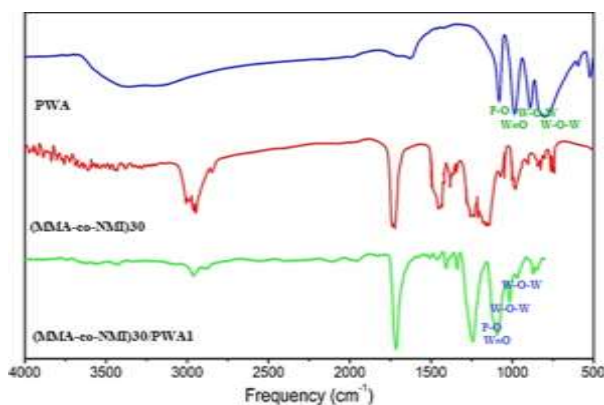


Fig. 4 FTIR spectra of PWA, poly(MMA-co-NMI)30 and poly(MMA-co-NMI)30/PWA1 membranes

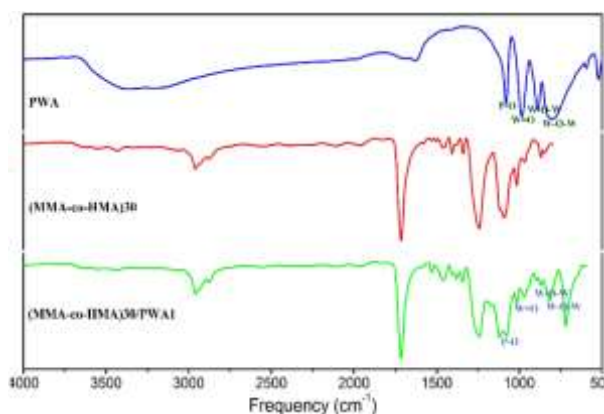


Fig. 5 FTIR spectra of PWA, poly(MMA-co-HMI)30 and poly(MMA-co-HMI)30/PWA1 membranes

FT-IR spectra of PWA, poly(MMA-co-HMI)30 and poly(MMA-co-HMI)30/PWA1 membranes are also presented in Fig. 5. The PWA spectrum shows absorption bands at about 1080 cm⁻¹ (P-O in central tetrahedral), 985 cm⁻¹ (terminal W=O), 890 cm⁻¹ and

814 cm⁻¹ (W-O-W) associated with the asymmetric vibrations in Keggin polyanions. Considering the

FTIR spectrum of poly(MMA-co-HMI) copolymer, there are some distinct peaks in 3180-3360 cm⁻¹, 2900-3100 cm⁻¹, 1720 cm⁻¹, 1544 cm⁻¹ and 1105 cm⁻¹ related to the stretching vibration of O-H, C-H, C=O,

C=C stretching and C-O stretching, respectively. Moreover, comparing the FTIR spectra of poly(MMA-co-HMI)30/PWA1 composite membrane with pure PWA indicates all main peaks (see Fig. 5).

However, some alteration in the shape and position of bands are observed due to the interaction between Keggin structure of PWA molecules and functional groups in the backbone of poly(MMA-co-HMI).

Table 2 Thermolysis information of copolymers

Sample	MMA%	HMI%	PWA%	Ti (°C)	T50 (°C)	Tmax (°C)	Residue (600°C) (%)	Tg (°C)
P(MMA-co-HMI)30	50	50	0	190	343	390	12	127
P(MMA-co-HMI)30/PWA1.5	50	50	1.5	151-240	345	465	20	135

4.2 Thermal Analyses

TGA and DTG curves of poly(MMA-co-HMI) membrane and poly(MMA-co-HMI)/PWA composite membrane at the temperature range of room temperature to 700 °C are shown in Fig. 6 and 7, respectively. Thermolysis data of polymers are also shown in Table 2.

Thermal degradation of poly(MMA-co-HMI)30 membrane occurred at one stage about (150°C), which is attributed to the elimination of residual solvent, moisture and oligomerization. Whereas, thermal degradation of poly(MMA-co-HMI)30/PWA1.5 membrane occurred at two stages. First, weight loss occurred at temperature about (151-240 °C) was associated with the loss of absorbed water, oligomerization of copolymer and evaporation of crystal water molecules of PWA. The initial decomposition temperatures (Ti) of copolymer with PWA content of 1.5% was about 240 °C. In the other words, it can be found that the composite membrane was thermally stable up to approximately about 240

°C showing enough stability for fuel cell applications at intermediate temperature (90–130 °C) [13].

The temperature corresponding to 50% weight loss (T50) is referred to structural decomposition and oligomerization of copolymers into the small parts. As observed, T50 of copolymer with 1.5% PWA particles was close to the copolymer having any PWA. The degradation at temperature of (345°C) is corresponding to the decomposition and oligomerization of copolymer combined with thermal degradation of copolymer, loss of all acidic protons and initial decomposition of the Keggin structure [13, 40]. Moreover, the temperatures of maximum degradation (Tmax) for two samples are displayed in DTG curves (see Table 2) declaring an increment by adding PWA into the membrane matrix. This result reveals a specific interaction contributing to enhancement in the thermal stability of composite membranes.

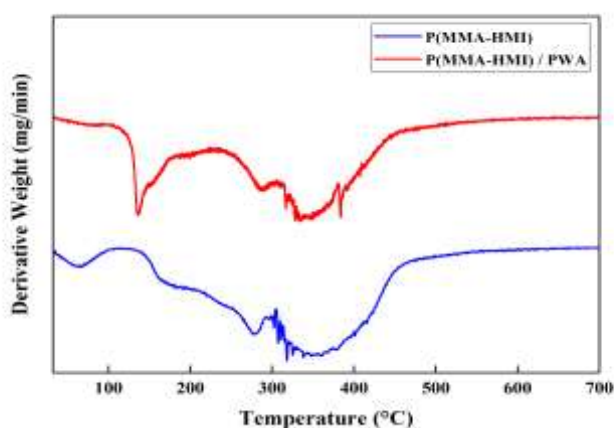


Fig. 6 TGA curves of the (MMA-co-HMI)30 membrane and (MMA-co-HMI)30 /PWA1.5 composite membrane

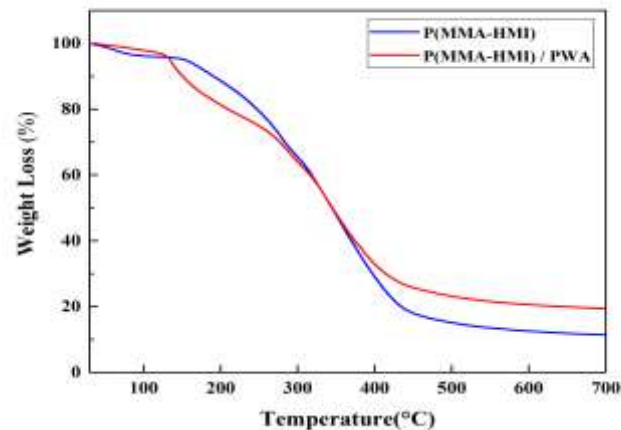


Fig.7 DTG diagram of (MMA-co-HMI)30 membrane and (MMA-co-HMI)30/PWA1.5 composite membrane

On the other hand, at the end of thermal degradation, the residual amount of poly(MMA-co-HMI)30 and poly(MMA-co-HMI)30/PWA1.5 at 600°C was about 12% and 20%, respectively. It can be indicated that the presence of PWA particles in copolymer has been influential on the copolymer thermal stability as a result of specific interactions occurred between OH groups of copolymer and functional groups of PWA. Composite of copolymers degraded at 600°C completely, but some parts of copolymers remained at the end of thermolysis. It exhibits that existence of more PWA units in the backbone has been effective

and poly(MMA-co-HMI)30/PWA1.5 composite copolymer offers better thermal stability than poly(MMA-co-HMI)30.

The DSC thermograms of poly(MMA-co-HMI)30 and poly(MMA-co-HMI)30/PWA1.5 membranes at the temperature range of room temperature to 700 °C are presented in Fig. 8. The T_g values of membranes without and with 1.5% of PWA are respectively 127 and 135°C, respectively. This difference is clearly due to the presence of 1.5% of PWA content in the composite membrane.

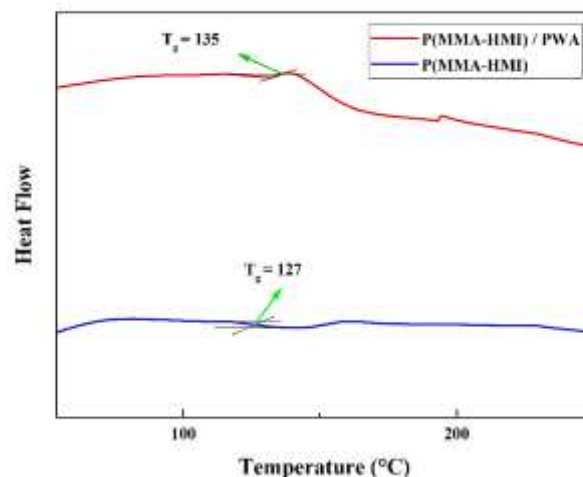


Fig. 8. DSC thermograms for (MMA-co-HMI)30 membrane and (MMA-co-HMI)30/PWA1.5 composite membrane

4.3 Ion Exchange Capacity and Water Uptake

The main feature of a proton exchange membrane is its ion exchange capacity (IEC). Experimental IEC estimated by calculation of free protons of added PWA are listed in Table 3. By comparing the

experimental values of IEC of membranes, it can be found that the IEC of poly(MMA-co-HMI)/PWA composite membranes is more than the IEC of poly(MMA-co-HMI) membrane. This may be related

to PWA additive into the copolymer matrix. The copolymers have not acidic property, and by the

addition of PWA, IEC was improved due to the increase in the acidity and H⁺ ions [34-36].

Table 3 Ion exchange capacity (IEC) of the membrane

Membrane Name	Copolymer	IEC(meq g ⁻¹)
Poly(MMA-co-HMI) 30		0.295
Poly(MMA-co-HMI) 30/PWA1	Poly(MMA-co-HMI)	0.347
Poly(MMA-co-HMI) 30/PWA1.5		0.464

On the other hand, the water uptake data of membranes at room temperature are shown in Table 4. In our experiments, poly(MMA-co-HMI)30/PWA1.5 membrane presented higher water uptake than poly(MMA-co-HMI)30 and poly(MMA-co-HMI)30/PWA1 composite membranes. Moreover, water absorption increased by adding a small amount of PWA content in the membrane samples (compare results of poly(MMA-co-HMI)30/PWA1.5 with poly(MMA-co-HMI)30/PWA1). This phenomenon may be explained by higher amount of PWA content in the

copolymer matrix. Since PWA has functional groups (OH and O₂) and water molecules, an addition of PWA to the mixture of copolymer results in more intermolecular hydrogen bonds which increases free volumes. These free volumes may trap more water molecules and increase water uptake in the membranes. Such interaction has been previously reported [13, 40]. There is no doubt that there is a direct relation between water uptake and proton exchange capability of membranes because of that it is expected that an improvement in the proton conductivity of membranes is observed as well.

Table 4 Water uptake of the membranes

Membrane Name	Copolymer	Water uptake (%)
Poly(MMA-co-HMI) 30		10.63
Poly(MMA-co-HMI) 30/PWA1	Poly(MMA-co-HMI)	10.90
Poly(MMA-co-HMI) 30/PWA1.5		12.91

4.4 Proton Conductivity

Results of measuring the proton conductivity of all prepared PEMFCs are tabulated in Table 5. As seen, the proton conductivity of poly(MMA-co-NMI) membrane increased from 1.0×10^{-2} to 1.6×10^{-2} S.cm⁻¹ as poly(MMA-co-NMI) concentration rose from 15 to 30 wt.%, respectively. This increment is due to the increased possible interaction of oxygen atoms of carbonyl group (C=O) groups as a proton acceptor with solvent molecules in the acid environment (Grotthuss mechanism) which is predicted through the formation of hydrogen bonds (H-bonding) [30]. Addition of 1 wt.% of PWA enhanced the proton conductivity of membranes to higher amounts of 1.5×10^{-2} S.cm⁻¹ (for poly(MMA-co-NMI)15) and

1.9×10^{-2} (for poly(MMA-co-NMI)30) as well. This increment is due to the increased possible interaction between (NO or NO₂ groups) of poly(MMA-co-NMI) with functional groups of PWA (W=O), proton transmission mechanism in the polymer electrolyte improves. Under the Grotthuss mechanism, the mobility of protons is determined by the formation of hydrogen bond between a hydronium ion (H₃O⁺, H₇O₃⁺, H₉O₄⁺, etc.) and another molecule or ion. On the other hand, proton might also transfer by diffusion of hydrolyzed water molecules in PWA structure. In this mechanism, proton diffuses through a vehicle such as H₂O (as H₃O⁺) [13, 40-45].

Considering the results of proton conductivity of prepared membranes with poly(MMA-co-HMI) copolymer and comparing the results with what was achieved for poly(MMA-co-NMI) membranes with the same concentration of copolymer reveal the higher efficiency of poly(MMA-co-HMI) membrane (see Fig. 9). This progress is due to the presence of

active sites (hydroxyl group) in the poly(MMA-co-HMI) matrix which increases the proton conductivity of the membrane. The hydroxyl groups are expected to have an important influence on the formation of strong hydrogen bonds in the proton exchange membrane.

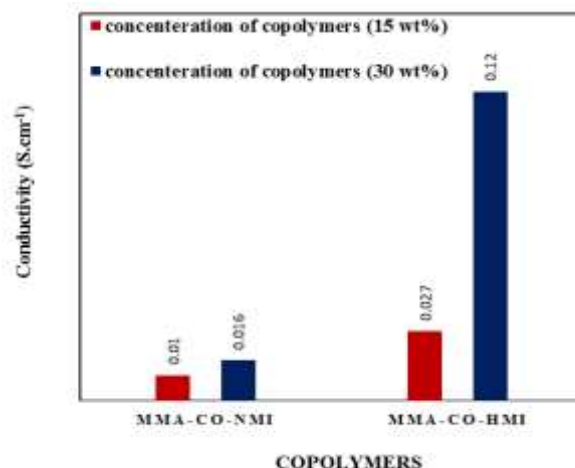


Fig.9. Effect of copolymer on the proton conductivity of membranes and poly(MMA-co-HMI)30 composite membranes

Moreover, the proton conductivity of membrane increased with an increment in the percentage of hydroxyl groups in the copolymer structure (compare conductivity results of poly(MMA-co-HMI)15 and poly(MMA-co-HMI)30 membranes in Table 5). Since the proton conductivity of membrane depends

on the path that proton passes and on the transport of charged carrier H^+ [13], in the poly(MMA-co-HMI) membrane protons also may be transferred by diffusion of hydrolyzed water molecules or hopping from one hydrolyzed ionic site to another across a hydrogen

Table 5 Results of proton conductivity of prepared membranes

Membrane Name	Copolymer	Copolymer amount (wt.%)	PWA (wt.%)	Proton conductivity (S.cm ⁻¹)
Poly(MMA-co-NMI)15	Poly(MMA-co-NMI)	15	0	0.01
Poly(MMA-co-NMI)15/PWA1			1	0.015
Poly(MMA-co-NMI)30		30	0	0.016
Poly(MMA-co-NMI)30/PWA1			1	0.019
Poly(MMA-co-HMI)15	Poly(MMA-co-HMI)	15	0	0.027
Poly(MMA-co-HMI)15/PWA0.5			0.5	0.05
Poly(MMA-co-HMI)15/PWA1			1	0.085
Poly(MMA-co-HMI)15/PWA1.5		1.5	0.091	
Poly(MMA-co-HMI)30		30	0	0.12
Poly(MMA-co-HMI)30/PWA1			1	0.18
Poly(MMA-co-HMI)30/PWA1.5			1.5	0.26

bond. Hence increasing the hydroxyl groups in poly(MMA-co-HMI)30 membrane would be beneficial in an improvement of membrane conductivity.

Results of proton conductivity of poly(MMA-co-HMI)15 and poly(MMA-co-HMI)30 composite membranes prepared with various concentrations of PWA are illustrated in Fig. 10.

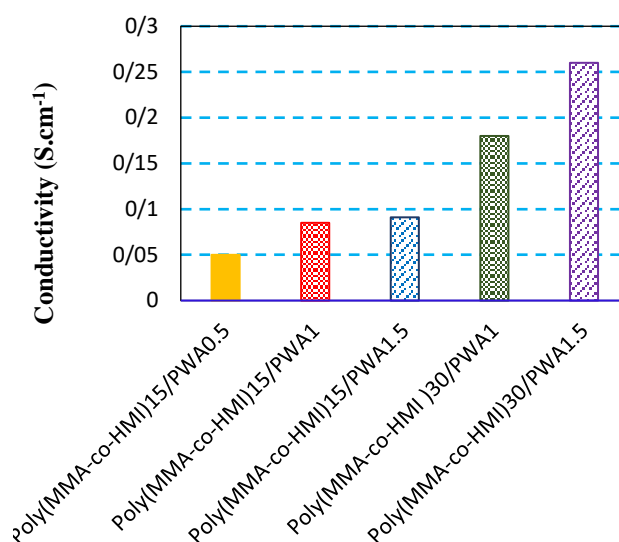


Fig. 10. Proton conductivity of poly(MMA-co-HMI)15 fabricated with different concentrations of PWA

As seen, addition of PWA into the poly(MMA-co-HMI) membrane matrix improved the conductivity performance of the membrane. This increment is more profound in poly(MMA-co-HMI)30 membranes prepared by PWA. Increasing the interaction between functional groups of copolymer and PWA improves the mobility of protons by creating active transport pathways. This proton mobility may occur by the formation of hydrogen bonds between H_3O^+ ions, O_2 clusters from PWA structure and OH, C=O functional groups from poly(MMA-co-HMI).

In order to investigate the composite membrane structure, SEM cross-section micrographs of poly(MMA-co-HMI) membrane prepared by 0 and 1.5 wt. % of PWA is shown in Fig. 11. The symmetric and dense structure of membranes are clearly observable in SEM images, and the cross-sectional micrographs show the excellent bonding structure between non-woven fibers and poly(MMA-co-

HMI)/PWA. Moreover, PWA particles are observed in some area in the membrane structure. Considering the results of poly(MMA-co-HMI)30 membranes prepared by different concentrations of PWA reveal that increasing the concentration of PWA in the membrane matrix raises the proton conductivity of membranes. Addition of 1 wt.% of PWA into the poly(MMA-co-HMI)30 membrane matrix successfully increased the proton conductivity to $1.8 \times 10^{-1} \text{ S.cm}^{-1}$. An increase in PWA to 1.5 wt.% (by just 50% increment compared to 1 wt.%) caused a considerable growth in proton conductivity to $2.6 \times 10^{-1} \text{ S.cm}^{-1}$ which was about 1.5 times more than that of poly(MMA-co-HMI)30/PWA1 membrane. This result proves that beneficial effect of PWA in improvement the proton conductivity of membrane. As it was mentioned, due to the interaction between functional groups of PWA (O, H_3O^+) and copolymers (C=O, NO and OH), proton transfer pathways increase based on the Vehicle mechanism and Grotthuss mechanism simultaneously.

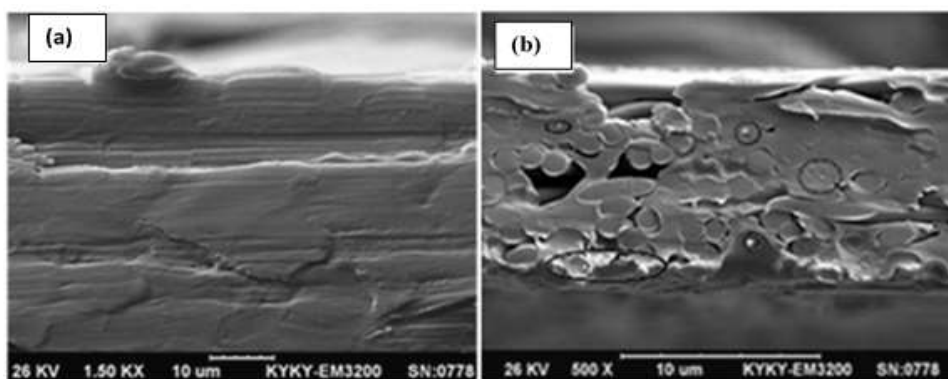


Fig. 11. SEM cross-section micrographs of (a) poly(MMA-co-HMI)30 and (b) poly(MMA-co-HMI)30/PWA1.5 membranes

5. Conclusions

In this study, poly(MMA-co-NMI) and poly(MMA-co-HMI) copolymers were prepared by the free radical polymerization of MMA with a new MI monomer containing phenyl and $-\text{NO}_2$ groups. Composite membranes prepared using synthesized copolymers and different concentrations of PWA as an additive. Generally, the results of proton conductivity showed an improvement in the characteristics of the conductive membrane prepared by poly(MMA-co-HMI) due to the OH groups in (MMA-co-HMI) copolymer which increased the movement of protons by causing proton transfer pathways through the formation of hydrogen bonds. Moreover, addition of PWA into the membrane matrix increased the proton conductivity of membranes because of formation of hydrogen bonds between H_3O^+ and O_2 clusters of PWA and functional groups of poly (MMA-co-HMI). Compared with (MMA-co-HMI)30 membrane,

(MMA-co-HMI)30/PWA1.5 composite membrane exhibited higher water uptake. Increasing the water uptake of the composite membranes by addition of PWA content may be explained on the basis of interaction between functional groups of PWA and active sites of copolymer via hydrogen bonding. By addition of PWA content to the composite membranes, IEC was improved due to the increase in the acidity and H^+ ion. TGA measurements showed that the composite membrane had a good thermal stability. The incorporation of PWA into copolymer not only enhanced the thermal stability of composite membrane, but also improved the conductivity. Addition of 1.5 wt.% of PWA into the poly(MMA-co-HMI)30 membrane matrix successfully increased the proton conductivity to $2.6 \times 10^{-1} \text{ S.cm}^{-1}$ which was about two and a half times more than that of poly(MMA-co-HMI)30 membrane.

References

- [1] J. Sutrisno, A. Fuchs, *ECS Trans.*, **28** (2010) 1.
- [2] Z. Zuo, Y. Fu and A. Manthiram, *J. Polymers*, **4** (2012) 1627.
- [3] R. Borup, J. Meyers, B. Pivovar, *Chem. Rev.*, **107** (2007) 3904.
- [4] M. Ahmad, B. Manuchehr, M. Paratoo, R. Reza, *J. Applied Chemistry*, **14** (1394) 92, in Persian.
- [5] H. Zhang, and P.K. Shen, *Chem. rev.*, **112** (2012) 2780.
- [6] M. Faraji, P. Derakhshi and K. Tahvildari, *J. Appl. Chem.*, **12** (2018) 31.

- [7] S. Bose, N. H. Kim, K. Lau and T. Kulla, *Prog. Polym. Sci.*, **36** (2011) 813.
- [8] Y. Devrim, S. Erkan, et al., *Int. J. Hydrogen Energy*, **34** (2009) 3467.
- [9] Y. Shao, G. Yin, Z. Wang, Y. Gao, *J. Power Sources*, **167** (2007) 235.
- [10] H. Gao, and K. Lian, *RSC Adv.*, **4**(2014) 33091.
- [11] F.J. Pinar, M.A. Rodrigo, et al., *J. Power Sources*, **274** (2015) 177.
- [12] D.J. Kim, , M.J. Jo and S.Y. Nam, *Ind. Eng. Chem.*, **21** (2015) 36.
- [13] L. Li, and Y. Wang, *J. power sources*, **162** (2006) 541.
- [14] L. Xu, F. Xu, F. Chen, et al., *J. Nanomaterials*, **20** (2012) 1.
- [15] B. Chen, G. Li, L. Wang, R. Chen, F. Yin, *Int. J. Hydrogen Energy*, **38** (2013) 7913.
- [16] T. Uma, and F. Yin, *Chem. phys. lett.*, **512** (2011) 104.
- [17] R. Kumar, and S.S. Sekhon, *Ionics*, **14** (2008) 509.
- [18] B. Singh, R. Kumar and S. Sekhon, *Solid State Ionics*, **176** (2005) 1577.
- [19] L. Othman, K.W. Chew and Z. Osman, *Ionics*, **13** (2007) 337.
- [20] S. Rajendran, V.S. Bama and M.R. Prabhu, *Ionics*, **16** (2010) 27.
- [21] Y. Liao, M. Rao, W. Li, et al., *Electrochim. Acta*, **54** (2009) 6396.
- [22] D. Shanmukaraj, G.X. Wang, R. Murugan, H., J.K. Liu, *Phys. Chem. of solids*, **69** (2008) 243.
- [23] Q. Xiao, Z. Li, D. Gao, H. Zhang., *J. Membrane Sci.*, **326** (2009) 260.
- [24] Y. Zhang, J. Li, et al., *J. Mater. Sci.*, **49** (2014) 3442.
- [25] H. Chung, C. Lee and H. Han, *Polymer*, **42** (2001) 319.
- [26] A. Gültek, T. Seckin, Y. Gökçen and S. Köytepe, *J. Appl. Sci.*, **3** (2015) 562.
- [27] N. Asano, M. Aoki, et al., *J. Am. Chem. Soc.*, **128** (2006) 1762.
- [28] C. Genies, R. Mercier, B. Sillion, N. Cornet, et al., *Polymer*, **42** (2001) 359.
- [29] E. Vallejo, C. Gavach, M. Pineri, et al., *J. Membrane Sci.*, **160** (1999) 127.
- [30] X. Li, L. Yan, and B. Yue, *Int. J. Hydrogen Energy*, **42** (2017) 515.
- [31] B.-K. Chen, J.-M. Wong, T.-Y. Wu, L.-C. Chen and I-Chao Shih, *Polymers*, **6** (2014) 2720.
- [32] Y.-L. Liu, *Polym. Chem.*, **3** (2012) 1373.
- [33] Tripathi, B.P. and V.K. Shahi, *Prog. Polym. Sci.*, **36** (2011) 945.
- [34] Y. Zhou, J. Yang, H. Su, et al., *J. Am. Chem. Soc.*, **136** (2014) 4954.
- [35] U.B. Mioč, S. Stojadinović and Z. Nedić, *Mater.*, **3** (2009) 110.
- [36] S.S. Madaeni, E. Rafiee, Z. Seyedzadeh, J. Barzin, *J. Polym. Eng.*, **30** (2010) 109.
- [37] V. Ramani, S. Swier, M. T. Shaw, R. A. Weiss and H. R. Kunz, *J. Electrochem. Soci.*, **155** (2008) 532.
- [38] Filipe N.D.C. Gomes, Fabiana M.T. Mendes and Mariana M.V.M. Souza, *Catal. Today*, **279** (2017) 296.
- [39] F. Atabaki, A. Abdolmaleki and A. Barati, *Colloid. Polym. Sci.*, **294** (2016) 455.
- [40] S.S. Madaeni, S. Amirinejad and M. Amirinejad, *J. Membrane sci.*, **380** (2011) 132
- [41] J. Jiang and O.M. Yaghi, *Chemi. rev.*, **115** (2015) 6966.

[42] Yamada, M. and I. Honma, J. Phys. Chem. B., **110** (2006) 20486.

[43] V. Rao, N. Kluy, W. Ju and U. Stimming, Handbook of Membrane Separations: Chemical, Pharmaceutical, Food and Biotechnological Applications Second Edition, Publication; Boca Raton, FL: CRC Press, c, 2015.

[44] S.J. Peighambardoust, S. Rowshanzamir and M. Amjadi, *Int. j. hydrogen energy*, **35** (2010) 9349.

[45] B. Fei, H. Lu, W. Chen, John H. Xin., **44** (2006) 2261.